




ARTICLE



Identification and in vivo functional investigation of a *HOMER2* nonstop variant causing hearing loss

Christel Vaché^{1,2}, Nicolas Cubedo³, Luke Mansard¹, Jérôme Sarniguet³, David Baux^{1,2}, Valérie Faugère¹, Corinne Baudoin¹, Melody Moclyn¹, Renaud Touraine⁴, Geneviève Lina-Granade⁵, Mireille Cossée^{1,6}, Anne Bergougoux^{1,6}, Vasiliki Kalatzis^{1,6}, Mireille Rossel^{3,7} and Anne-Françoise Roux^{1,2,7}

© The Author(s), under exclusive licence to European Society of Human Genetics 2023

DFNA68 is a rare subtype of autosomal dominant nonsyndromic hearing impairment caused by heterozygous alterations in the *HOMER2* gene. To date, only 5 pathogenic or likely pathogenic coding variants, including two missense substitutions (c.188 C > T and c.587 G > C), a single base pair duplication (c.840dupC) and two short deletions (c.592_597delACCACA and c.832_836delCCTCA) have been described in 5 families. In this study, we report a novel *HOMER2* variation, identified by massively parallel sequencing, in a Sicilian family suffering from progressive dominant hearing loss over 3 generations. This novel alteration is a nonstop substitution (c.1064 A > G) that converts the translational termination codon (TAG) of the gene into a tryptophan codon (TGG) and is predicted to extend the *HOMER2* protein by 10 amino acids. RNA analyses from the proband suggested that *HOMER2* transcripts carrying the nonstop variant escaped the non-stop decay pathway. Finally, in vivo studies using a zebrafish animal model and behavioral tests clearly established the deleterious impact of this novel *HOMER2* alteration on hearing function. This study identifies the fourth causal variation responsible for *DFNA68* and describes a simple in vivo approach to assess the pathogenicity of candidate *HOMER2* variants.

European Journal of Human Genetics (2023) 31:834–840; <https://doi.org/10.1038/s41431-023-01374-0>

INTRODUCTION

Approximately 20–30% of hereditary nonsyndromic hearing loss (NSHL) cases diagnosed in infancy and early childhood present an autosomal dominant inheritance pattern (ADNSHL) [1]. For the vast majority of these cases, the HL is described as postlingual, bilateral and progressive. To date at least 51 causal genes have been identified (Hereditary Hearing Loss Homepage; <https://hereditaryhearingloss.org/>; accessed in May, 2022) and one of them is *HOMER2* (OMIM*604799).

The *HOMER2* gene is located on chromosome 15, spans 103.7 kb (UCSC Genome browser; <http://genome.ucsc.edu/>; accessed in May, 2022), and encodes several isoforms of the HOMER homolog 2 protein, including two long isoforms (*HOMER2a*: 343 aa, NP_004830.2 and *HOMER2b*: 354 aa, NP_955362.1) due to alternative splicing (NM_004839.4 and NM_199330.2, respectively). These *HOMER2* isoforms belong to the HOMER family of scaffolded proteins (encoded as short and long isoforms by alternative splicing of the *HOMER1*, *HOMER2* and *HOMER3* genes), which are involved in Ca²⁺ homeostasis, cytoskeletal organization and synaptic plasticity (for review see [2]). The long HOMER proteins are all characterized by the presence of two main domains: (i) a conserved N-terminal Enabled Vasodilator-stimulated phosphoprotein Homology 1 (EVH1) domain that interacts with proline-rich sequences, (ii) a

C-terminal domain, comprising a coiled-coiled region with a CDC42-binding domain and two leucine zipper motifs, responsible for multimerization between HOMER family members and interaction with the CDC42 small GTPase [3].

Azaiez et al. [4] were the first to establish the causality of a heterozygous missense *HOMER2* variation, NM_199330.2:c.587 G > C, p.(Arg196Pro) (published as NM_004839.4:c.554 G > C, p.(Arg185Pro)) in a dominantly inherited form of NSHL (*DFNA68*). Thereafter, three other *HOMER2* pathogenic heterozygous variants were identified in three families suffering from ADNSHL: the NM_199330.2:c.840dupC, p.(Met281HisfsTer9) variant (published as c.840_841insC) in a large Chinese family [5], the NM_199330.2:c.592_597delACCACA, p.(Thr198_Thr199del) variant in an Italian family [6], and the NM_199330.2:c.832_836delCCTCA, p.(Pro278AlafsTer10) variant in a Spanish family [7]. Another variant (NM_199330.2:c.188 C > T, p.(Pro63Leu)) reported in an Iranian family with dominant deafness was also described [8] and assumed as likely pathogenic by the authors although the variation was of uncertain significance when applying the ACMG criteria.

In this article, we have identified a new *HOMER2* variant segregating in a large Sicilian family suffering from ADNSHL. This alteration, which was not reported in databases, consists of a nonstop substitution, a very rare variant class. RNA analysis from

¹Molecular Genetics Laboratory, Univ Montpellier, CHU Montpellier, Montpellier, France. ²Institute for Neurosciences of Montpellier (INM), Univ Montpellier, Inserm, Montpellier, France. ³MMDN, Univ Montpellier, EPHE, INSERM, Montpellier, France. ⁴Department of Genetics, CHU Hopital Nord, Saint-Etienne, France. ⁵Department of Oto-Rhino-Laryngology, Head and Neck Surgery, Edouard Herriot Hospital, Hospices Civils de Lyon, Lyon University Hospital, Lyon, France. ⁶PhyMedExp, Univ Montpellier, INSERM, CNRS, Montpellier, France. ⁷These authors jointly supervised this work: Mireille Rossel, Anne-Françoise Roux. ✉email: christel.vache@inserm.fr

Received: 13 March 2023 Revised: 18 April 2023 Accepted: 25 April 2023

Published online: 12 May 2023

the proband's peripheral blood sample demonstrated that it results in the production of abnormal RNA transcripts with a 3' coding sequence extension. Finally, its deleterious effect on hearing was established using zebrafish behavioral tests. With this study we expanded the genotype spectrum associated with *DFNA68* and developed a simple zebrafish experiment to test future candidate pathogenic *HOMER2* variants.

MATERIALS AND METHODS

Patients

A forty-eight-year-old female (index case) and her fifteen-year-old daughter, both suffering from progressive bilateral nonsyndromic hearing loss, were referred to our laboratory for genetic analyses. For each individual, pure tone audiometry, in a frequency range of 250–8000 Hz, was performed to evaluate the severity of their hearing loss in accordance with the recommendations of the International Bureau for Audiophonology (<https://www.biap.org/en/recommendations/recommendations/tc-02-classification/213-rec-02-1-en-audiometric-classification-of-hearing-impairments/file>). In addition, a family history questionnaire was completed by the clinicians. Informed consent for genetic analyses was obtained from all participants or their legal representatives. Approval was obtained by the Institutional Review Board (IRB) of CHU de Montpellier: (2018_IRB-MTP_05-05 obtained on the 15th June 2018).

Sequencing and validation

DNA from each participant was isolated from peripheral blood samples using standard procedures. Massively parallel sequencing (MPS) was performed with a hearing loss gene panel on an Illumina® MiniSeq sequencer (Illumina, San Diego, CA, USA). The workflow used to identify candidate pathogenic variations has been already described [9] and the 84 screened genes are listed in Supplementary Table 1. This approach included a copy-number variant analysis using the MobiCNV algorithm (<https://github.com/mobidic/MobiCNV>) and a direct visualization of the sequenced reads with the Integrative Genomics Viewer (IGV) software (v2.7.2) [10]. Whole exome sequencing (WES) libraries were prepared using the KAPA® HyperPlus kit (Roche, Madison, WI, USA) according to the KAPA® HyperCap v3.0 workflow. Whole exome enrichment was then performed using the KAPA® HyperExome probes (~43 Mb capture target size) and an Illumina® NextSeq 500 instrument (Illumina) was used for sequencing. Samples were analyzed using an in-house pipeline (MobiDL, <https://github.com/mobidic/MobiDL>), which performs the secondary and tertiary analyses, and uses BWA [11] as aligner and both GATK HaplotypeCaller [12] and Google DeepVariant [13] as variant callers. Furthermore, copy-number variation (CNV) was assessed using the GATK4 CNV calling module and a pipeline (https://gitlab.univ-nantes.fr/benjamin.co/sv-exome/-/tree/add_vcf_support) based on the GATK recommendations. Variant filtering was based on: (i) a dominant mode of inheritance, (ii) a genotype/phenotype correlation and (iii) a minor allele frequency (MAF) threshold of 0.1%.

Sanger sequencing or MPS were performed in order to validate identified variants and build a comprehensive familial genetic profile. Primer sequences used for PCR-Sanger sequencing are listed in Supplementary Table 2.

In silico analysis and data availability

The reference sequences used in this study were NM_199330.2, NM_153676.3 and NM_194248.2. for the *HOMER2*, *USH1C* and *OTOF* genes, respectively. Functional consequences of variants of interest were evaluated using the online variant interpretation platform Mobidetails [14] (<https://mobidetails-iurc-montp-inserm.fr/MD/>; accessed in March, 2023). The Human Gene Mutation Database (HGMD® Professional 2020.3; <https://portal.biobase-international.com>) and the Deafness Variation Database (DVD) (<https://deafnessvariationdatabase.org/>) were also consulted (accessed in March, 2023). The Human Genome Variation Society recommendations [15] v20.05 (<http://varnomen.hgvs.org/>) were followed for the description of the variants.

The newly identified variant was classified using the Intervar web server (<http://wintervar.wglab.org/>) in accordance with the adapted ACMG/AMP guidelines for variant interpretation in the context of hearing loss [16] and deposited in the Leiden Open Variation Database Global Variome Shared Instance (LOVD GVShared, individuals #00411547 to #00411552).

cDNA analysis of *HOMER2*

Total RNA from the proband and a control was isolated from peripheral blood samples collected in PAXgene™ Blood RNA Tubes using the Nucleo Spin® RNA II isolation kit (Macherey-Nagel, Düren, Germany). RNA quality and concentration were estimated with a 4200 TapeStation system (Agilent Technologies, Santa Clara, USA). RNA samples were used as templates for cDNA synthesis using the SuperScript™ III Reverse Transcriptase (Invitrogen, Cergy-Pontoise, France) and PCR amplifications were performed with *HOMER2*-specific primers (Supplementary Table 2). PCR products were size-separated on agarose gel and Sanger sequenced.

Zebrafish husbandry

This study was conducted in accordance with the recommendations of INSERM, Montpellier University and the European Convention for the Protection of Animals used for Experimental and Scientific Purposes. The zebrafish Tg(pou4f3:gap43-GFP)s356t transgenic line, re-defined later as *Brn3c:mGFP* [17], was maintained according to recommended Federation of European Laboratory Animal Science Associations (FELASA) procedures on a 14:10 h light/dark photoperiod at 28 °C [18]. Embryos were obtained from natural spawning and incubated in a water tank at 28 °C. Embryos and larvae were staged by days post-fertilization (dpf).

mRNA synthesis and injection

The pShuttle™ Gateway® PLUS ORF clone for *HOMER2* (GC-H5096) and its mutated version (*HOMER2*, c.1064 A > G, 30 bp 5'-GGCTGGCCGAGGCC-CAGGCCCGCCCGTGA-3' extension) were purchased from GeneCopoeia™ (GeneCopoeia, Rockville, MD, USA). The ORF sequences were subcloned into the expression vector pCS2+ (gift from Marc Kirschner (Addgene plasmid # 17095; <http://n2t.net/addgene:17095>; RRID: Addgene_17095)) using the Gateway™ LR Clonase™ II Enzyme Mix (Invitrogen, Carlsbad, CA, USA). The pCS2+ mCherry expression vector [19] (gift from Georges Lutfalla; DIMNP, CNRS, University of Montpellier, Montpellier, France) was also used.

Transcription was carried out using the mMESSAGE mMACHINE™ T7 or SP6 transcription kit (Invitrogen) for *HOMER2* wild type, *HOMER2* mutated or mCherry RNA synthesis, respectively. RNA quality and concentration were assessed by electrophoresis and spectrophotometry (NanoDrop One/One^C, Thermo Fisher Scientific, Waltham, MA, USA). A dilution range was performed to determine the optimal mRNA quantity that allowed a good ratio of toxicity/phenotype analysis. Therefore, 80 pg of *HOMER2* RNA (wild type sequence: A1064-RNA or mutated sequence: G1064-RNA) were co-injected with 50 pg of mCherry RNA, 1 nL at the one- to two-cell stage. Twenty-four hours after microinjection, mCherry fluorescence was used as a quality control of injection and translation; all negative embryos were discarded.

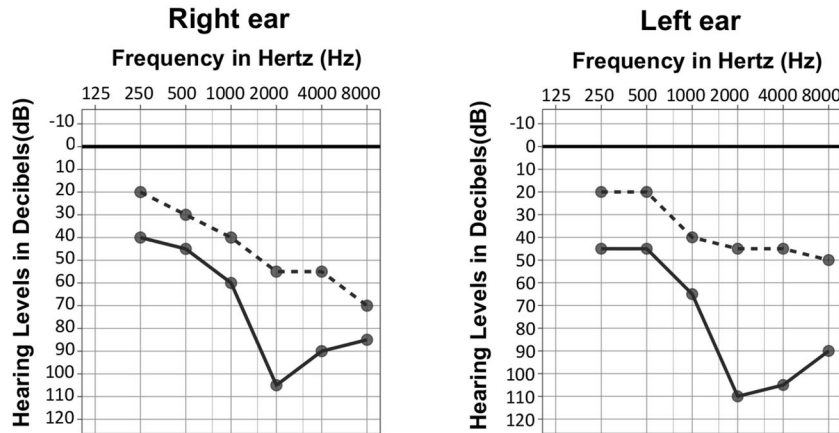
Acoustic startle response (ASR) test

At 5 dpf, zebrafish larvae with normal morphology were transferred into a 96-well plate with 300 µl of water per well and placed into a Zebrabox® (ViewPoint, Lissieu, France). In the device, larvae in the plate were isolated from environmental surrounding noise. After a 30 min period of adaptation, larvae were submitted to 3 noise stimulations (70 dB, 400 Hz, 1 s per stimulus, 5 min apart). The study was conducted in light condition and zebrafish activity was quantified using the quantization mode of Zebralab® software (ViewPoint), as previously described [20]. The quantity of movements during the entire experiment was measured for each larva. Baseline activity levels were subtracted from the activity levels during the sound stimulations (10 s pre-stimulus period before each stimulation) in order to normalize the values. The activity for the 3 stimuli were pooled into 1 s time to assess ASR.

Visual motor response (VMR) assay

Following the ASR test, each 96-well plate was then used to assess the locomotor activity of the larvae in response to visual stimuli. This test quantifies the activity of zebrafish larvae in response to light changes using infrared tracking system. The VMR protocol consisted of a 30 min dark-adaptation period followed by two periods, each composed of 10 min of brightness (100% of light intensity) and 10 min of darkness, the duration of the whole protocol was 70 min. Zebrafish activity was quantified with the Zebralab® software and data were analyzed using 1 min time bins to assess the VMR.

a



b

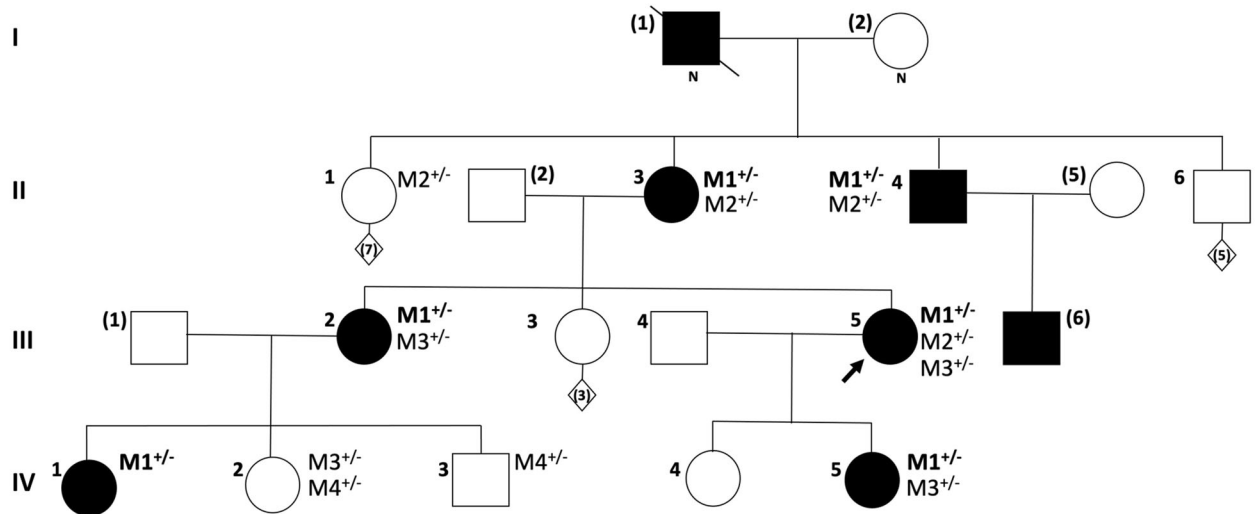


Fig. 1 Audiograms of the proband and her daughter, pedigree chart of the family and segregation of the identified variants. **a** Superimposed audiograms of the patient at the age of 28 years old (solid line) and her daughter at the age of 13 years old (dotted line) showing bilateral downward-sloping severe and mild 1st degree hearing loss, respectively. **b** Pedigree of the proband's family with segregation of the heterozygous variants when present: *HOMER2*, c.1064 A > G (M1 ±); *USH1C*, c.778 G > T (M2 ±); *OTOF*, c.327 + 5 G > T (M3 ±) and *USH1C*, c.496 + 1 G > A (M4 ±). The proband (III.5) is indicated by a black arrow, filled symbols denote affected individuals, brackets indicate a person not involved in the study.

Statistical analyses

Statistical analyses were performed using Prism™ v8.3 software (GraphPad, San Diego, CA, USA). A chi-square contingency test was performed to analyze the ASR results. Other data were analyzed with non-parametric Mann-Whitney test and were represented as mean ± SEM. Asterisks indicate statistical significance: **p* value < 0.05, ***p* value < 0.01, ****p* value < 0.001 and *****p* value < 0.0001.

RESULTS

Clinical findings

The proband of this study (III.5) was a 48-year-old female suffering from progressive sensorineural nonsyndromic hearing loss (NSHL). The clinical diagnosis of its deafness was made at the age of 7 years, but an earlier onset was presumed by the patient in the light of her educational difficulties. At the age of 28 years,

audiometric assessment revealed a bilateral downward-sloping severe 1st degree HL according to the BIAP recommendations (Fig. 1a). When she was 47 years old, she was fitted with hearing aids. Her daughter (IV.5) was diagnosed at the age of 3 years and an air conduction test performed at age 13 years showed a bilateral downward-sloping mild 1st degree HL (Fig. 1a). The family anamnesis revealed 6 additional affected members over 4 generations (I.1, II.3, II.4, III.2, III.6 and IV), consistent with an autosomal dominant inheritance pattern of the pathology (Fig. 1b).

DNA and RNA analysis

Following our laboratory diagnostic approach, massive parallel sequencing (MPS) analysis using a panel of 84 deafness-causing genes was firstly performed in the proband (III.5) to identify

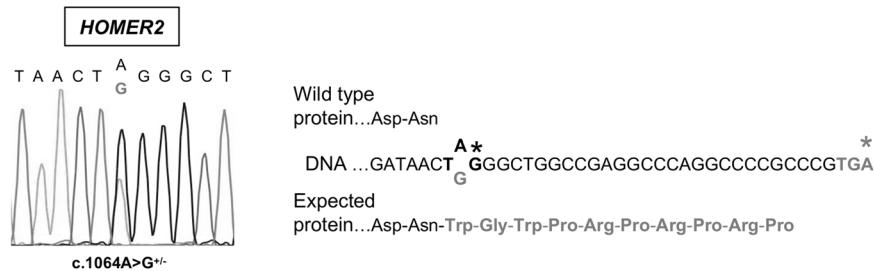


Fig. 2 Identification of the *HOMER2* variant. On the left, Sanger sequencing electropherogram of the heterozygous c.1064 A > G *HOMER2* variant segregating with the autosomal dominant nonsyndromic hearing loss in the proband's family. On the right, consequences of the variant at the DNA and protein (expected) levels. The native termination (stop) codon is indicated with bold black font and black star whereas the subsequent in-frame one is indicated with bold gray font and gray star. The 10 amino-acid residues extension of the expected protein is also shown.

candidate pathogenic variants. This screening strategy highlighted the presence of a *HOMER2* A > G transition (c.1064 A > G) in the heterozygous state (Fig. 2). This variant occurred within the translational termination (stop) codon (TAG) of the gene and changed it to a tryptophan codon (TGG). According to the *HOMER2* human reference genome sequence, a downstream in-frame stop codon was detected, leading to a predicted 10 amino acids C-terminal extension of the protein (Fig. 2). This substitution was absent from all the interrogated databases and was considered as a variant of uncertain significance according to the ACMG/AMP hearing loss guidelines. Sanger sequencing validated the genotype of the proband and revealed that her affected daughter was also a heterozygous carrier (Fig. 1b).

In addition, MPS data analysis highlighted two other variants, both in the heterozygous state, in two genes implicated in hearing loss (Supplementary Table S3). The first one was a previously described pathogenic variation (c.778 G > T, p.(Glu260Ter)) in *USH1C* [21], a gene responsible for both nonsyndromic (OMIM#602092) and syndromic (OMIM#276904) recessive deafness. The second one was an intronic transversion (c.327 + 5 G > T) in *OTOF*, a gene associated with recessive NSHL (OMIM#601071). This last substitution was present in the Genome Aggregation Database (gnomAD v2.1.1) with a minor allele frequency (MAF) of 0.13% in European (Finnish) and was referred in ClinVar (Variation ID: 335462) as a variant of uncertain significance or a likely benign variation. Splicing predictions obtained with the MaxEntScan and SpliceAI tools were in favor of a deleterious effect of the variant via an alteration of the donor consensus splice site of exon 4. By contrast, the deep neural network SpliceAI did not predict this adverse event but indicated a moderate increase in the probability that a cryptic donor splice site, located 48-bp upstream of the natural donor splice site, could be used. These two *USH1C* and *OTOF* variants were validated by Sanger sequencing in the proband. The *OTOF* variation was also present in the proband's daughter (Fig. 1b).

In order to exclude the implication of a non-explored DFNA gene in the familial hearing loss, whole exome sequencing (WES) was then carried out with DNA samples from four affected (II.4, III.5, IV.1 and IV.5) and one unaffected (III.4) individuals. After filtering for MAF, genotype/phenotype correlation and a dominant mode of inheritance, the only selected variant was the *HOMER2* nonstop substitution. Further segregation of this variant in the family showed it was only detected in the affected members (Fig. 1b).

As the *USH1C* and *OTOF* variants identified in the proband could be important for the other family members in a context of genetic counselling, a segregation analysis was additionally performed with Sanger sequencing or MPS. Unexpectedly, this analysis highlighted the presence of another well-known *USH1C* pathogenic variant (c.496 + 1 G > A; ClinVar variation ID: 371732) in the unaffected IV.2 and IV.3 individuals, presumably inherited from their father III.1 (Fig. 1b and Supplementary Table S3).

Finally, the consequence of the c.1064 A > G *HOMER2* variation at the RNA level was assessed by RT-PCR study on total RNA extracted from proband's blood sample. Sanger sequencing revealed that *HOMER2* transcripts carrying the c.1064 A > G were present and not subject to a major degradation by the non-stop decay pathway (Fig. 3).

Zebrafish behavioral assays

In order to determine the pathogenicity of the *HOMER2* nonstop variant identified in this study we performed *in vivo* assays using a zebrafish model expressing human *HOMER2* protein when injected with synthesized *HOMER2* wildtype RNA (A1064-RNA) or mutated *HOMER2* RNA (G1064-RNA) (Fig. 4a and Supplementary Fig.1a).

A behavioral test, based on recording the acoustic startle response (ASR) was firstly conducted to assess a potential hearing defect in 5 dpf larvae injected with G1064-RNA. The larval locomotor activity in response to noise stimuli above noise background was tracked and differences in the ratio responsive to non-responsive larvae were estimated between the 3 groups: non-injected controls (NI), injected with the wildtype A1064-RNA (A1064) and injected with the mutant G1064-RNA (G1064). ASR data analyses, from three independent tests, highlighted a significant decrease in the number of responsive larvae exposed to noise (70 db, 400 HZ) in the G1064 group compared to the A1064 group ($p < 0.0001$), whereas no significance difference was observed between the A1064 and NI groups (Fig. 4b).

To exclude a locomotion impairment due to the G1064-RNA injection, a visual motor response (VMR) assay was systematically performed after each ASR experimentation (Fig. 4c). The locomotor reflex was induced by flash of light, independently to acoustic stimulation. Statistical analyses of data obtained from all VMR tests (Fig. 4c) indicated that the locomotor activity of larvae from the G1064 group was not impacted by the overexpression of the mutated *HOMER2* RNA in both ON phases and OFF phases, in comparison with the A1064 group.

As a complement to these behavioral tests, β -actin normalized *HOMER2* RNA levels and ear diameters from injected 3 dpf larvae (Supplementary Fig. 1b, c) were also studied. For these two analyses, no significant difference was observed between the A1064 and G1064 groups.

Altogether, these results obtained from zebrafish experimentations characterized the c.1064 A > G *HOMER2* substitution as a causal variant responsible for hearing loss.

DISCUSSION

Single-nucleotide pathogenic substitutions that change stop codons into sense codons, termed nonstop variants (also known as no-stop, stop-loss or readthrough variations), are an extremely rare type of alteration (387 nonstop variants among 278,993 single

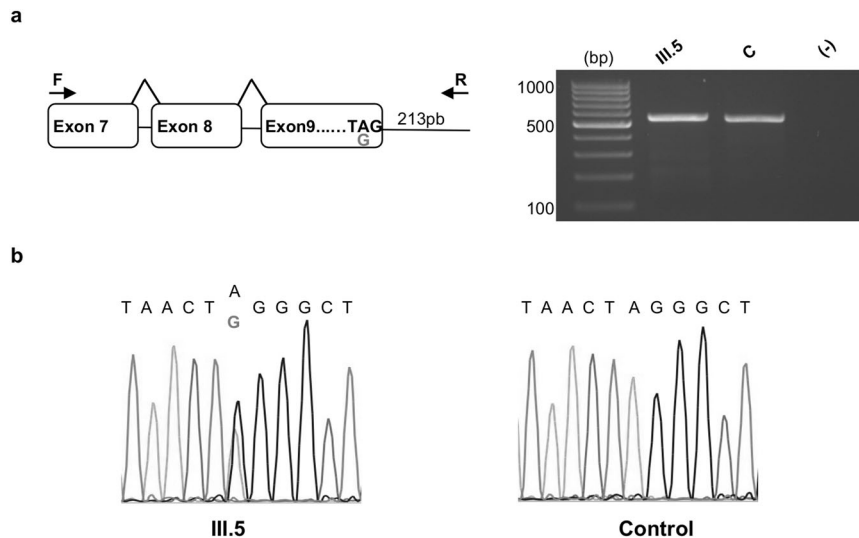


Fig. 3 Consequence of the c.1064 A > G *HOMER2* variant on the RNA. **a** Schematic representation of the study and agarose gel electrophoresis of the RT-PCR products from the proband (III.5) and a control. Primers (forward: F, reverse: R) were indicated with black arrows **(b)** Sanger sequencing electropherograms of the *HOMER2* transcripts from the proband and a control.

pathogenic nucleotide substitutions reported in the HGMD database (accessed in March, 2023)). In this study we identified a *HOMER2* nonstop variation segregating with the hearing loss (HL) phenotype described in a large Sicilian family. This result was obtained by massively parallel sequencing of a HL gene panel, confirmed by a whole exome sequencing analysis and validated by Sanger sequencing.

To date only four pathogenic *HOMER2* variants have been clearly associated with *DFNA68*, a missense and a two small deletions in three European families [4, 6, 7] and a single nucleotide duplication in a Chinese family [5]. In these families, all affected individuals suffering from bilateral progressive nonsyndromic hearing loss (NSHL) affecting preferentially the high frequencies with an onset (when indicated) in the first decade of life (7–9 years old), which is consistent with the clinical data collected from the family described herein. It was reported that the severity of the hearing impairment could be variant-dependent [5, 7], but due to the limited number of cases a fine genotype/phenotype correlation remains difficult to establish. Concerning the fifth reported variant, c.188 C > T, no family history or clinical data was reported [8].

Nonstop pathogenic alterations can lead to: (i) mRNA degradation due to activation of the non-stop decay (NSD) pathway in response to the presence of stalled or collided ribosomes [22], (ii) degradation of the mutated protein by protein quality control mechanisms [23, 24] or (iii) functional alteration of the mutated protein [25, 26]. As results obtained from studies on animal models [4] strongly suggest that the pathogenicity of *HOMER2* variants implicated in *DFNA68* is not due to haploinsufficiency, a massive *HOMER2* mRNA degradation by NSD linked to the nonstop variant appeared unlikely. To test this hypothesis, RT-PCR analyses were performed and confirmed that transcripts carrying the *HOMER2* nonstop variation were not a major target of the NSD system. This result was in accordance with data obtained from a meta-analysis [27], which suggested that alternative stop codons in close proximity to the mutated stop codons (0–49 nucleotides downstream) were not subject to NSD.

In order to validate the pathogenicity of the c.1064 A > G *HOMER2* substitution, we then performed in vivo behavioral tests on zebrafish larvae injected with wild type or mutated *HOMER2* RNA. The zebrafish model has been already used by Azaiez et al. [4] to study the impact of the c.587 G > C *HOMER2* variant. In this previous publication, the effect of the variant was determined by

measurements of the otic capsule area in 3 dpf larvae while in vivo behavioral tests were conducted in mice. In our study, we performed the behavioral assays on zebrafish larvae at 5 dpf, using the ASR and VMR conventional tests, which is a much more rapid and straightforward model as we were able to directly compare wild type and variant phenotypes. The ASR test revealed a clear decrease in larval activity when injected with the mutated *HOMER2* RNA, whereas the VMR assay did not revealed any change in their locomotor capacity, highlighting a hearing impairment. This result was also validated by a western blot experiment detecting human *HOMER2* proteins in injected embryos and a qRT-PCR study of the *HOMER2* RNA that confirmed the integrity of the injected RNAs in larvae at 3 dpf. In order to compare our results to those obtained by Azaiez et al. [4], we also measured the ear diameters of 3 dpf larvae injected with wild type or mutated *HOMER2* RNAs, and showed that contrary to the c.587 G > C variant, the nonstop alteration did not impair the morphology of the ears.

Taking into consideration all these results, and according to ACMG/AMP guidelines, we classified the c.1064 A > G *HOMER2* transition as a class V pathogenic variant.

The exact molecular mechanism involved in the pathogenicity of the *HOMER2* nonstop variant has not been determined. A dominant-negative effect on the wild type protein or a gain-of-function have been discussed for the previously identified pathogenic alterations. In the case of the nonstop variant, the 10 amino-acids protein extension could inhibit the multimerization process, which occurs via the C-terminal domains of the proteins or could compete for other partner proteins resulting in a dominant-negative effect.

In summary, in this article, we identified a new *HOMER2* variation associated with progressive dominant NSHL. This variant consisting of a nonstop substitution, a very rare type of pathogenic variation, expands the mutational spectrum of the *HOMER2* gene. Identification of this pathogenic variant and 3 other alterations in 2 deafness-causing genes will have important consequences for the proband's family concerning medical care and genetic counseling. Furthermore, this study highlights the major importance of developing functional tests to unambiguously characterize the pathogenicity of a variants of uncertain significance. Finally, we believe that using zebrafish animal model and simple behavioral assays, such as ASR and VMR, should be considered and encouraged in a molecular diagnostic strategy when necessary.

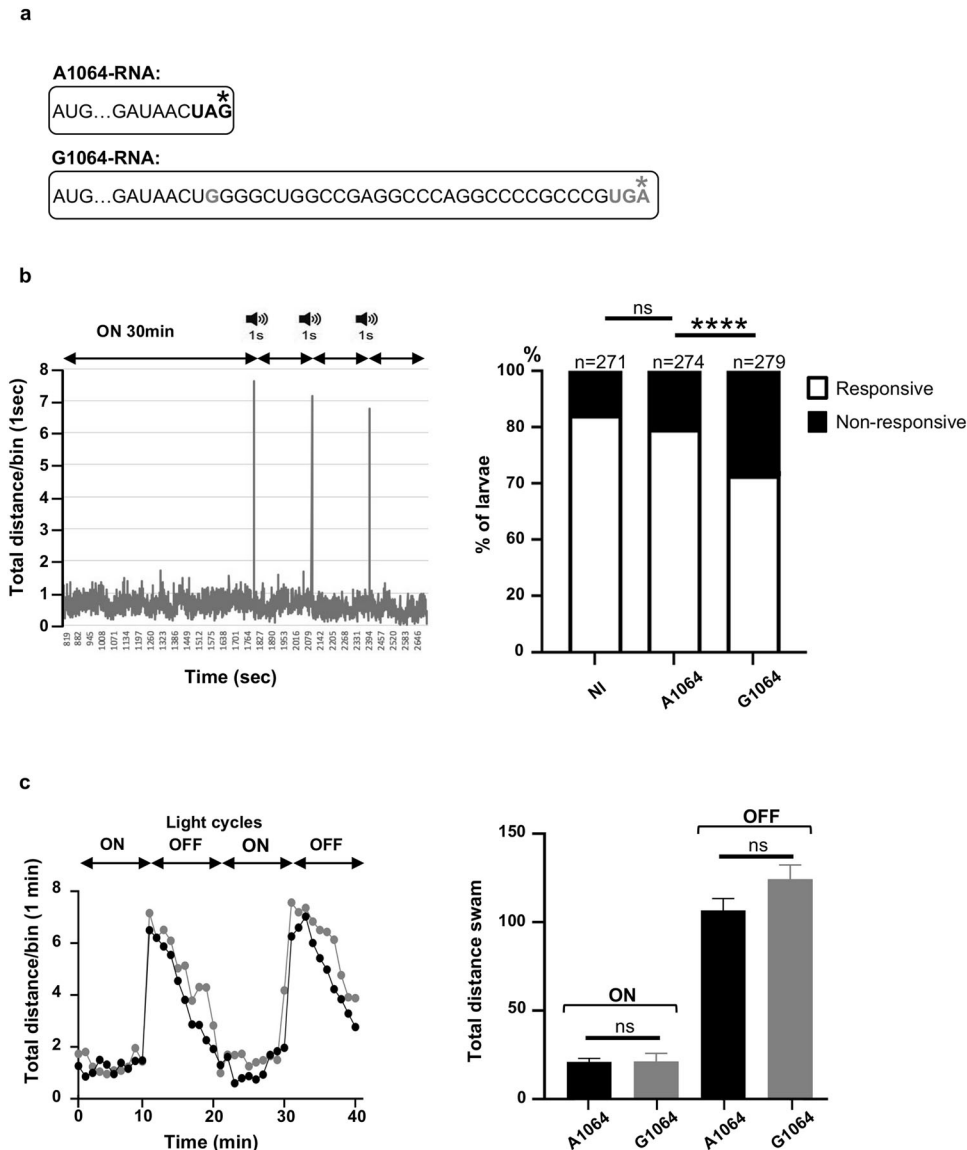


Fig. 4 Behavioral responses of larvae at 5 dpf. **a** Schematic representation of the 3' end of the 2 full length in vitro synthesized RNAs (A1064-RNA and G1064-RNA). **b** Acoustic startle response (ASR) assay. Left chart: profiles of control non-injected larvae with normal response for each acoustic stimulation. Right chart: percentage values of responsive and non-responsive larvae from non-injected control. Percentage values of responsive and non-responsive larvae from the non-injected group (NI), A1064-RNA injected group (A1064) and G1064-RNA injected group (G1064) are displayed in a stacked column chart. The number of larvae in each group is indicated (n). **** p value < 0.0001; ns: not significant. **c** Visual motor response (VMR) test. Left chart: profiles of larvae from the A1064 group (black dots) and the G1064 group (gray dots) focused on the two ON/OFF sessions of the VMR test. Average of the total distance traveled every 1 min bin is plotted for each group. Right chart: average distances swam by each group during the two pooled ON or OFF sessions. Differences between the two groups is not significant (ns).

DATA AVAILABILITY

The data that support this study are available from the corresponding author upon reasonable request. The variants, individual and phenotype described in this paper is available to the LOVD GVShared, Individual ID number #00411547 to #00411552 (e.g., <https://databases.lovd.nl/shared/individuals/00411547>).

REFERENCES

- Morton NE. Genetic epidemiology of hearing impairment. *Ann N. Y Acad. Sci.* 1991;630:16–31.
- Shiraishi-Yamaguchi Y, Furuichi T. The Homer family proteins. *Genome Biol.* 2007;8:206.
- Shiraishi-Yamaguchi Y, Sato Y, Sakai R, Mizutani A, Knöpfel T, Mori N, et al. Interaction of Cupidin/Homer2 with two actin cytoskeletal regulators, Cdc42 small GTPase and Drebrin, in dendritic spines. *BMC Neurosci.* 2009;10:25.
- Azaiez H, Decker AR, Booth KT, Simpson AC, Shearer AE, Huygen PLM, et al. HOMER2, a stereociliary scaffolding protein, is essential for normal hearing in humans and mice. *PLoS Genet.* 2015;11:e1005137.
- Lu X, Wang Q, Gu H, Zhang X, Qi Y, Liu Y. Whole exome sequencing identified a second pathogenic variant in HOMER2 for autosomal dominant non-syndromic deafness. *Clin Genet.* 2018;94:419–28.
- Morgan A, Lenarduzzi S, Spedicati B, Cattaruzzi E, Murru FM, Pelliccione G, et al. Lights and Shadows in the Genetics of Syndromic and Non-Syndromic Hearing Loss in the Italian Population. *Genes (Basel).* 2020;11:1237.
- Lachgar M, Morin M, Villamar M, Del Castillo I, Moreno-Pelayo MÁ. A Novel Truncating Mutation in HOMER2 Causes Nonsyndromic Progressive DFNA68 Hearing Loss in a Spanish Family. *Genes (Basel).* 2021;12:411.
- Noorian S, Khonsari NM, Savad S, Hakak-Zargar B, Voth T, Kabir K. Whole-Exome Sequencing in Idiopathic Short Stature: Rare Mutations Affecting Growth. *J Pediatr Genet.* 2021;10:284–91.

9. Baux D, Vaché C, Blanchet C, Willems M, Baudoin C, Moclyn M, et al. Combined genetic approaches yield a 48% diagnostic rate in a large cohort of French hearing-impaired patients. *Sci Rep.* 2017;7:16783.
10. Thorvaldsdóttir H, Robinson JT, Mesirov JP. Integrative Genomics Viewer (IGV): high-performance genomics data visualization and exploration. *Brief Bioinform.* 2013;14:178–92.
11. Li H, Durbin R. Fast and accurate long-read alignment with Burrows-Wheeler transform. *Bioinformatics* 2010;26:589–95.
12. Auwera G van der, O'Connor BD. *Genomics in the cloud: using Docker, GATK, and WDL in Terra.* First edition. Sebastopol, CA: O'Reilly Media; 2020. p. 467.
13. Poplin R, Chang PC, Alexander D, Schwartz S, Colthurst T, Ku A, et al. A universal SNP and small-indel variant caller using deep neural networks. *Nat Biotechnol.* 2018;36:983–7.
14. Baux D, Van Goethem C, Ardouin O, Guignard T, Bergougnot A, Koenig M, et al. MobiDetails: online DNA variants interpretation. *Eur J Hum Genet.* 2021;29:356–60.
15. den Dunnen JT, Dalgleish R, Maglott DR, Hart RK, Greenblatt MS, McGowan-Jordan J, et al. HGVS Recommendations for the Description of Sequence Variants: 2016 Update. *Hum Mutat.* 2016;37:564–9.
16. Oza AM, DiStefano MT, Hemphill SE, Cushman BJ, Grant AR, Siegert RK, et al. Expert specification of the ACMG/AMP variant interpretation guidelines for genetic hearing loss. *Hum Mutat.* 2018;39:1593–613.
17. DeCarvalho AC, Cappendijk SLT, Fadool JM. Developmental expression of the POU domain transcription factor Brn-3b (Pou4f2) in the lateral line and visual system of zebrafish. *Dev Dyn.* 2004;229:869–76.
18. Aleström P, D'Angelo L, Midtlyng PJ, Schorderet DF, Schulte-Merker S, Sohm F, et al. Zebrafish: Housing and husbandry recommendations. *Lab Anim.* 2020;54:213–24.
19. Hirsinger E, Carvalho JE, Chevalier C, Lutfalla G, Nicolas JF, Peyriéras N, et al. Expression of fluorescent proteins in Branchiostoma lanceolatum by mRNA injection into unfertilized oocytes. *J Vis Exp.* 2015;95:52042.
20. Crouzier L, Richard EM, Diez C, Alzaem H, Denus M, Cubedo N, et al. Morphological, behavioral and cellular analyses revealed different phenotypes in Wolfram syndrome wfs1a and wfs1b zebrafish mutant lines. *Hum Mol Genet.* 2022;31:2711–27.
21. Abdi S, Bahloul A, Behlouli A, Hardelin JP, Makrelouf M, Boudjelida K, et al. Diversity of the Genes Implicated in Algerian Patients Affected by Usher Syndrome. *PLoS One.* 2016;11:e0161893.
22. Powers KT, Szeto JYA, Schaffitzel C. New insights into no-go, non-stop and nonsense-mediated mRNA decay complexes. *Curr Opin Struct Biol.* 2020;65:110–8.
23. Torres-Torronteras J, Rodriguez-Palmero A, Pinós T, Accarino A, Andreu AL, Pintos-Morell G, et al. A novel nonstop mutation in TYMP does not induce nonstop mRNA decay in a MNGIE patient with severe neuropathy. *Hum Mutat.* 2011;32:E2061–2068.
24. Pang S, Wang W, Rich B, David R, Chang YT, Carbanaru G, et al. A novel nonstop mutation in the stop codon and a novel missense mutation in the type II 3beta-hydroxysteroid dehydrogenase (3beta-HSD) gene causing, respectively, non-classic and classic 3beta-HSD deficiency congenital adrenal hyperplasia. *J Clin Endocrinol Metab.* 2002;87:2556–63.
25. Sun J, Hao Z, Luo H, He C, Mei L, Liu Y, et al. Functional analysis of a nonstop mutation in MITF gene identified in a patient with Waardenburg syndrome type 2. *J Hum Genet.* 2017;62:703–9.
26. Bock AS, Günther S, Mohr J, Goldberg LV, Jahic A, Klisch C, et al. A nonstop variant in REEP1 causes peripheral neuropathy by unmasking a 3'UTR-encoded, aggregation-inducing motif. *Hum Mutat.* 2018;39:193–6.
27. Hamby SE, Thomas NST, Cooper DN, Chuzhanova N. A meta-analysis of single base-pair substitutions in translational termination codons ("nonstop" mutations) that cause human inherited disease. *Hum Genom.* 2011;5:241–64.

ACKNOWLEDGEMENTS

We are grateful to the family members who contributed to this study. We thank Dr Yoan Arribat, University of Lausanne (Switzerland), for his help with Gateway cloning and Dr Benjamin Cogné, CHU of Nantes (France), for the GATK pipeline.

AUTHOR CONTRIBUTIONS

Conceptualization, CV, MR, and A-FR; Human molecular genetic investigations, CV, LM, VF, CB, and MM; Clinical investigations, RT and GL-N; Zebrafish investigations, CV, NC, JS, and MR; Software, DB, Writing—original draft preparation, CV and MR; Writing—review and editing, A-FR, VK, MC, and AB. Supervision, A-FR and MR. All authors have read and agreed to the published version of the paper.

FUNDING

This work was partially funded by the association SOS Rétinite France and the French Agency of BioMedicine (AOR AMP 2017).

COMPETING INTERESTS

The authors declare no competing interests.

ETHICS APPROVAL

The institutional review board (IRB) of CHU de Montpellier approved the experimental protocol (2018_IRB-MTP_05-05 obtained on the 15th June 2018). The zebrafish study was conducted in accordance with the recommendations of INSERM, Montpellier University and the European Convention for the Protection of Animals used for Experimental and Scientific Purposes.

ADDITIONAL INFORMATION

Supplementary information The online version contains supplementary material available at <https://doi.org/10.1038/s41431-023-01374-0>.

Correspondence and requests for materials should be addressed to Christel Vaché.

Reprints and permission information is available at <http://www.nature.com/reprints>

Publisher's note Springer Nature remains neutral with regard to jurisdictional claims in published maps and institutional affiliations.

Springer Nature or its licensor (e.g. a society or other partner) holds exclusive rights to this article under a publishing agreement with the author(s) or other rightsholder(s); author self-archiving of the accepted manuscript version of this article is solely governed by the terms of such publishing agreement and applicable law.